Inhibition of Epidermal Growth Factor Receptor Activation Is Associated With Improved Diabetic Nephropathy and Insulin Resistance in Type 2 Diabetes

Zhilian Li,[1,2,3] Yan Li,[2,3,4] Jessica M. Overstreet,[2,3] Sungjin Chung,[2,3] Aolei Niu,[2,3] Xiaofeng Fan,[2,3] Suwan Wang,[2,3] Yinqiu Wang,[2,3] Ming-Zhi Zhang,[2,3] and Raymond C. Harris[2,3,5]

Diabetes 2018;67:1847–1857 | https://doi.org/10.2337/db17-1513

Previous studies by us and others have indicated that renal epidermal growth factor receptors (EGFR) are activated in models of diabetic nephropathy (DN) and that inhibition of EGFR activity protects against progressive DN in type 1 diabetes. In this study we examined whether inhibition of EGFR activation would affect the development of DN in a mouse model of accelerated type 2 diabetes (BKS *db/db* with endothelial nitric oxide knockout [eNOS$^{-/-}$*db/db*]). eNOS$^{-/-}$*db/db* mice received vehicle or erlotinib, an inhibitor of EGFR tyrosine kinase activity, beginning at 8 weeks of age and were sacrificed at 20 weeks of age. In addition, genetic models inhibiting EGFR activity (*waved 2*) and transforming growth factor-α (*waved 1*) were studied in this model of DN in type 2 diabetes. Compared with vehicle-treated mice, erlotinib-treated animals had less albuminuria and glomerulosclerosis, less podocyte loss, and smaller amounts of renal profibrotic and fibrotic components. Erlotinib treatment decreased renal oxidative stress, macrophage and T-lymphocyte infiltration, and the production of proinflammatory cytokines. Erlotinib treatment also preserved pancreas function, and these mice had higher blood insulin levels at 20 weeks, decreased basal blood glucose levels, increased glucose tolerance and insulin sensitivity, and increased blood levels of adiponectin compared with vehicle-treated mice. Similar to the aforementioned results, both *waved 1* and *waved 2* diabetic mice also had attenuated DN, preserved pancreas function, and decreased basal blood glucose levels. In this mouse model of accelerated DN, inhibition of EGFR signaling led to increased longevity.

Diabetic nephropathy (DN) is one of the most prominent microvascular complications of diabetes and is a major source of morbidity and mortality. Both the incidence and the prevalence of DN continue to rise. The vast majority of incident and prevalent cases of DN are secondary to type 2 (obesity-related) diabetes. With the global rise in the incidence of obesity, an increasing incidence of DN also is being reported worldwide.

The underlying mechanisms predisposing to development and progression of DN are an area of active investigation. Studies with experimental animals have identified a number of cytokines, hormones, and intracellular signaling pathways that may be involved in either the development or the progression of DN (1). Angiotensin II and transforming growth factor (TGF)-β are known to play central roles in mediating the progressive glomerulopathy and tubulointerstitial fibrosis that characterize DN (2,3), and renin-angiotensin-aldosterone system (RAAS) blockade is the only "specific" intervention currently available for the treatment of patients with DN. Studies show that RAAS inhibition slows—but does not always prevent—progressive injury in DN (4).

[1]Guangdong General Hospital, Guangdong Academy of Medical Sciences, Guangdong, China
[2]Division of Nephrology and Hypertension, Department of Medicine, Vanderbilt University School of Medicine, Nashville, TN
[3]Vanderbilt Center for Kidney Disease, Vanderbilt University School of Medicine, Nashville, TN
[4]Shanghai Ninth People's Hospital, Shanghai Jiao Tong University School of Medicine, Shanghai, China
[5]Department of Veterans Affairs, Nashville, TN

Corresponding author: Raymond C. Harris, ray.harris@vanderbilt.edu, or Ming-Zhi Zhang, ming-zhi.zhang@vanderbilt.edu.

Received 14 December 2017 and accepted 18 June 2018.

This article contains Supplementary Data online at http://diabetes.diabetesjournals.org/lookup/suppl/doi:10.2337/db17-1513/-/DC1.

Z.L. and Y.L. contributed equally to this work.

Epidermal growth factor receptor (EGFR) is a member of the ErbB receptor (ErbB) family, which consists of four transmembrane receptors belonging to the receptor tyrosine kinase superfamily and includes EGFR (ErbB1/HER1), ErbB2/Neu/HER2, ErbB3/HER3, and ErbB4/HER4 (5–7). Among the four ErbB, EGFR is the prototypical receptor and is widely expressed in mammalian kidney, including in the glomerulus, proximal tubule, and cortical and medullary collecting ducts (8–11). Receptor activation leads to phosphorylation of specific tyrosine residues within the cytoplasmic tail. These phosphorylated residues serve as docking sites for a variety of signaling molecules whose recruitment leads to the activation of intracellular pathways, including the mitogen-activated protein kinase, Janus kinase/STAT, src kinase, and phosphoinositide 3-kinase pathways, which control cell proliferation, differentiation, and apoptosis (5–7). We previously reported EGFR activation in experimental models of type 1 diabetes in mice and found that erlotinib, an EGFR tyrosine kinase inhibitor, inhibited EGFR activation and markedly inhibited the development of DN (11–14). The study presented here investigated the role of EGFR signaling in mediating progressive glomerular and tubulointerstitial injury in type 2 DN. We were surprised to find that inhibition of EGFR tyrosine kidney activity not only retards the progression of DN but also ameliorates insulin resistance.

RESEARCH DESIGN AND METHODS

Animal Studies

All animal experiments were performed in accordance with the guidelines of the Institutional Animal Care and Use Committee of Vanderbilt University. *db/db* mice with endothelial nitric oxide knockout (eNOS$^{-/-}$*db/db*) on a C57BLKS/J (BKS) background were generated as described previously (15). Genotyping was performed by PCR. Twenty eNOS$^{-/-}$*db/db* mice (8 weeks old) were treated daily with either the vehicle (water) or erlotinib, an EGFR tyrosine kinase inhibitor, at 80 mg/kg/day, via gastric gavage for both. Mice were euthanized at 20 weeks of age. An additional set of mice began treatment with the vehicle (n = 8 mice) or erlotinib (n = 8 mice) at 8 weeks of age and continued treatment until 40 weeks of age or death. Both *waved 1* mice harboring a null mutation of TGF-α, an EGFR ligand (stock no. 000004), and *waved 2* mice harboring a point mutation in the EGFR gene, with resultant loss of most of its tyrosine kinase activity (stock no. 025148), were purchased from The Jackson Laboratory. These mice were crossed with eNOS$^{-/-}$*db/*+ mice to eventually get *wa1/*+;eNOS$^{-/-}$*db/db* (control) and *wa1/wa1*;eNOS$^{-/-}$*db/db* (*waved 1*) mice, as well as *wa2/*+;eNOS$^{-/-}$*db/db* (control) and *wa2/wa2*;eNOS$^{-/-}$*db/db* (*waved 2*) mice.

Measurements of Blood Glucose, Insulin, and Urinary Albumin Excretion

Fasting blood glucose was evaluated with a B-Glucose Analyzer (HemoCue, Lake Forest, CA) through the use of blood samples taken from the saphenous veins of conscious mice at 2:00 P.M. after they had been deprived of food for 6 h, beginning at 8:00 A.M. Plasma insulin was measured at the Vanderbilt Diabetes Research and Training Center by using radioimmunoassay. Urinary albumin and creatinine excretion was determined with Albuwell M ELISA kits (Exocell, Philadelphia, PA). Albuminuria was expressed as the ratio of urinary albumin concentration to creatinine concentration (micrograms per milligram).

Intraperitoneal Glucose Tolerance Test

Mice were deprived of food overnight (16 h), after which a glucose solution (100 mg/mL) was injected intraperitoneally at a dose of 2 mg/g body wt (200 μL/10 g body wt). Then blood glucose was measured 0, 15, 30, 90, 120, and 150 min after glucose injection.

Insulin Tolerance Test

Mice were deprived of food for 6 h (8:00 A.M. to 2:00 P.M.), after which insulin was injected intraperitoneally at a dose of 3 μg/kg body wt (60 μL/10 g body wt). Then blood glucose was monitored 0, 15, 30, 45, 60, 75, and 90 min after insulin administration. Insulin sensitivity was expressed as a percentage of baseline blood glucose.

Measurement of Blood Pressure by Using a Tail Cuff and Carotid Catheterization

Mice were anesthetized with ketamine (80 μg/g; Fort Dodge Laboratories) and inactin (8 μg/g; BYK Additives & Instruments), administered through intraperitoneal injection, and placed on a temperature-controlled pad. After tracheostomy, phycoerythrin 10 tubing was inserted into the right carotid artery. The catheter was tunneled under the skin, exteriorized, secured at the back of the neck, filled with heparinized saline, and sealed. The catheterized mice were housed individually and trained three times before blood pressure was measured with a blood pressure analyzer (Micro-Med, Inc.) (16). Systolic blood pressure was also measured with a tail-cuff microphonic manometer (16).

Measurement of Plasma Adiponectin

Plasma adiponectin concentration was measured using an EZMADP-60K Mouse Adiponectin ELISA Kit (Millipore), according to the manufacturer's instructions.

Determination of Urinary F2-Isoprostane

Mice were trained three times in metabolic cages (Braintree Scientific, Inc., Braintree, MA) before urine was collected continuously for 16 h. A single mouse was placed in a metabolic cage overnight and then returned to its original cage for 2 days before the next training period. The metabolic cages were humidified to minimize the evaporation of the urine samples when 16-h urine samples were collected. F2-isoprostanes, which are prostaglandin F2–like compounds, have been recognized as sensitive and specific biomarkers of oxidative stress. Urinary F2-isoprostane levels were determined by negative-ion gas chromatography–mass spectrometry (17).

Histologic Analysis

Kidney sections stained with periodic acid Schiff were evaluated for glomerulosclerosis; investigators were blinded to the identity of the various groups. A semiquantitative index was used to evaluate the degree of glomerulosclerosis. Each glomerulus in a single section was graded from 0 to 4, where 0 represents no lesion; 1 represents sclerosis involving <25% of the glomerular tuft area; 2 represents sclerosis involving 25–50%; 3 represents sclerosis involving 50–75%; and 4 represents sclerosis involving >75% of the glomerular tuft area (12).

Antibodies

Goat anti–phosphorylated EGFR (Tyr 1173, SC-12351) and rabbit anti–phosphorylated EGFR (Tyr845, SC-23420-R) were purchased from Santa Cruz Biotechnology. Goat anti-EGFR (E1282) and mouse anti–α-smooth muscle actin (a marker of myofibroblasts; A5228) were from Sigma-Aldrich (St. Louis, MO). Rabbit anti–phosphorylated extracellular signal–regulated kinase (ERK; 4370S), anti-p62 (5114), and mouse anti–CHOP (2895) were from Cell Signaling Technology. Guinea pig anti–insulin antibody (ab7842) and rabbit anti–Wilms tumor protein (a marker of podocytes; ab89901) were from Abcam. Rat anti–mouse F4/80 (MCA497R) and rat anti–mouse CD8α (MCA2694) were purchased from AbD Serotec (now Bio-Rad Laboratories). Rabbit antimurine collagen type I (600-401-103-01) was from Rockland Immunochemicals, Inc. Rat anti–kidney injury molecule-1 and mouse anti–4-hydroxynonenal (a marker of oxidative stress; no. 198960) were from R&D Systems.

RNA Isolation and Quantitative RT-PCR

Total RNA were isolated from tissues using TRIzol reagent (Invitrogen). Quantitative RT-PCR was performed using TaqMan real-time PCR (7900HT; Applied Biosystems). The master mix and all gene probes were also purchased from Applied Biosystems. The probes used in the experiments included mouse S18 (Mm02601778), collagen I (Col1a1; Mm00801666), collagen III (col3a1; Mm01254476), fibronectin 1 (Fn1; Mm01256744), connective tissue growth factor (CTGF; Mm01192933), TGF-β (Mm00441726), F4/80 (Emr1; Mm00802529), CD3 (Cd3d; Mm00442746), interleukin (IL)-6 (Mm00446190), interferon (INF)-γ (Mm01168134), inducible nitric oxide synthase (iNOS; Mm00440502), tumor necrosis factor (TNF)-α (Mm99999068), AdipoR1 (Mm01291331), and AdipoR2 (Mm01184032).

Masson Trichrome Staining and Picrosirius Red Staining

To evaluate kidney fibrosis, Masson trichrome staining and Picrosirius Red staining were performed according to the protocols provided by the manufacturer (Sigma-Aldrich).

Immunofluorescence/Immunohistochemistry Staining

The animals were anesthetized with Nembutal Sodium (70 mg/kg i.p.) and exsanguinated with heparinized saline (2 units/mL heparin in 0.9% NaCl) through a transcardial aortic cannula to minimize coagulation. After one kidney was removed and stored at −80°C for immunoblotting and quantitative PCR, the other kidney was perfused with 3.7% formaldehyde, 10 mmol/L sodium *m*-periodate, 40 mmol/L phosphate buffer, and 1% acetic acid for immunohistochemical and immunofluorescent staining; this solution provides excellent preservation of tissue structure and antigenicity and mRNA (18). The fixed kidney was dehydrated through a graded series of ethanol concentrations, embedded in paraffin, cut into sections (4 μm thick), and mounted on glass slides. The sections were immunostained as described in a previous report (12).

Micrography

Bright-field images from a Leitz Orthoplan microscope with an Optronics DEI-750 three-chip red-green-blue color video camera were digitized with the BIOQUANT TCW system and these digitized images were saved as tiff files. Contrast and color level were adjusted (with Adobe Photoshop) within the entire image; that is, no region- or object-specific editing or enhancements were performed.

Statistics

All values are presented as the mean ± SEM (for bar graphs) or the mean ± SD (for univariate scatter plots). We used the Fisher exact test, ANOVA, and Bonferroni *t* test for statistical analysis.

RESULTS

All erlotinib-induced changes described occurred in comparison with the vehicle-treated group. The eNOS$^{-/-}$*db/db* mouse model is an accelerated model of DN, and these mice develop significant functional and structural injury during the first 20 weeks of life (15). Inhibition of EGFR activation by erlotinib, an EGFR tyrosine kinase inhibitor, in the kidney of eNOS$^{-/-}$*db/db* mice was confirmed by inhibition of EGFR phosphorylation and inhibition of activation of ERK1/2 (Fig. 1). As indicated in Fig. 2*A*, at 8 weeks of age the mice had significant albuminuria, but administration of erlotinib prevented further increases in the severity of

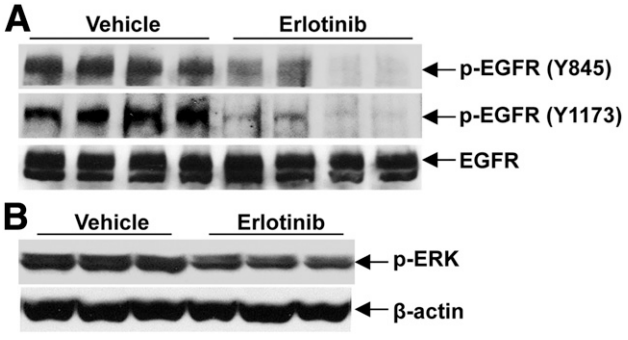

Figure 1—Erlotinib effectively inhibited EGFR tyrosine kinase activity in eNOS$^{-/-}$*db/db* mice. *A*: Erlotinib inhibited the levels of phosphorylated EGFR (p-EGFR) at different tyrosine residues. *B*: Erlotinib treatment led to decreased levels of phosphorylated extracellular signal–regulated kinase (p-ERK), a downstream signaling target of EGFR activation.

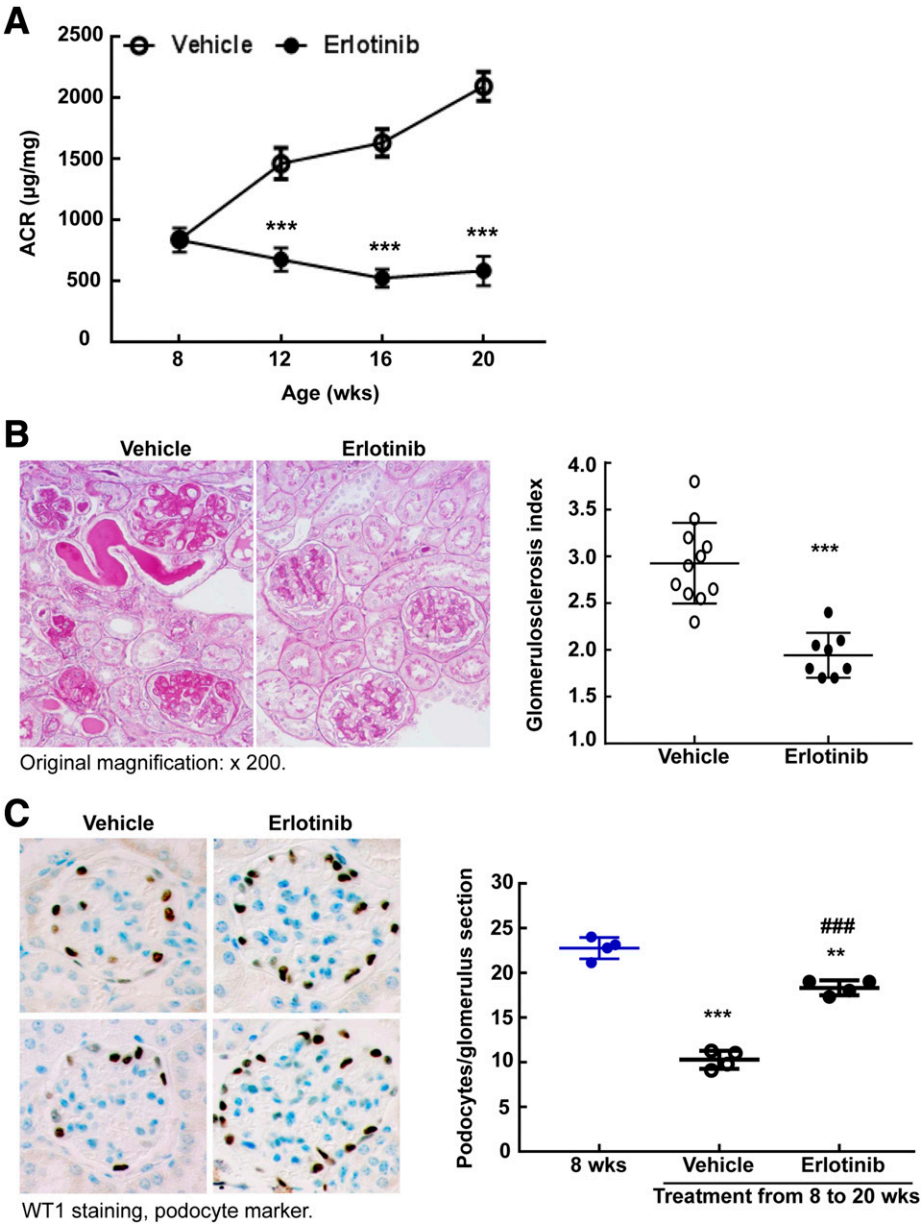

Figure 2—Erlotinib treatment prevented the progression of DN. *A*: Erlotinib treatment prevented the progressive increases in albuminuria that occurred in vehicle-treated eNOS$^{-/-}$*db/db* mice from 8 to 20 weeks. ***$P < 0.001$ vs. the corresponding vehicle group (n = 10 mice in each group). *B*: Erlotinib treatment decreased glomerulosclerosis as indicated by period acid Schiff staining. Right panel shows quantitative glomerular sclerosis index. ***$P < 0.001$; n = 11 mice in the vehicle-treated group and n = 8 mice in the erlotinib-treated group. Original magnification ×200. *C*: Erlotinib treatment from 8 to 20 weeks markedly slowed the loss of podocytes in eNOS$^{-/-}$*db/db* mice, as indicated by brown WT1 staining, a marker of podocyte nuclei. Blue indicates the nuclei of other cells. Right panel shows podocyte number in each glomerulus section from different groups. **$P < 0.01$, ***$P < 0.001$ vs. baseline (8 weeks old); ###$P < 0.001$ vs. the vehicle-treated group (n = 4 mice in each group). Original magnification ×400. ARC, albumin-to-creatinine ratio; WT1, Wilms tumor protein.

albuminuria (urinary albumin-to-creatinine ratio at 20 weeks: 588 ± 120 vs. 2,098 ± 117 μg/mg vehicle; $P < 0.001$ [n = 10 mice in each group]). Unlike our previous studies with RAAS inhibition in this model (19), erlotinib administration did not decrease blood pressure as measured with a tail cuff and carotid catheterization (Supplementary Fig. 1).

Protection against DN imparted by erlotinib was also indicated by decreased glomerulosclerosis (Fig. 2*B*). Podocyte number was relatively preserved in response to erlotinib treatment (podocytes per glomerular section at 8 weeks: 22.77 ± 0.60; at 20 weeks: 18.33 ± 0.41; in response to vehicle: 10.28 ± 0.41; $P < 0.001$ [n = 4 mice in each group]) (Fig. 2*C* and Supplementary Fig. 2). Furthermore, tubulointerstitial injury and fibrosis were decreased, as indicated by deceased expression of kidney injury molecule-1 (a marker of proximal tubule injury) (Fig. 3*A*); decreased Sirius Red, α-smooth muscle actin, and collagen I staining; and decreased expression of mRNA for components

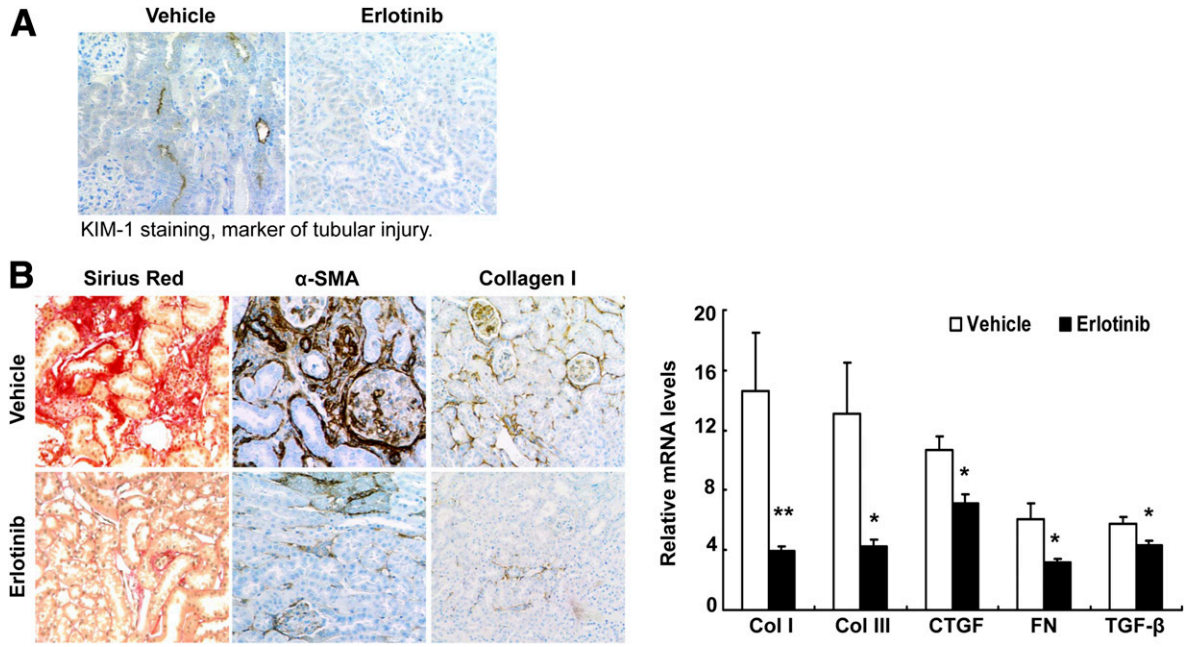

Figure 3—Erlotinib treatment decreased tubular injury and tubulointerstitial fibrosis. *A*: Erlotinib treatment decreased proximal tubule injury, as indicated by a reduction of the expression of kidney injury marker-1 (KIM-1), a marker of tubular injury. Original magnification ×300. *B*: Erlotinib treatment in mice from 8 to 20 weeks of age attenuated renal tubulointerstitial fibrosis, as indicated by decreases in Sirius Red staining, α-smooth muscle actin (α-SMA), and collagen I (Col I) immunostaining (left; original magnification ×200), and by decreases in mRNA levels of Col I, collagen III (Col III), connective tissue growth factor (CTGF), fibronectin (FN), and TGF-β (right). *$P < 0.05$, **$P < 0.01$ ($n = 8$ mice in the vehicle-treated group and $n = 6$ mice in the erlotinib-treated group).

of fibrosis (collagens I and III, fibronectin) and profibrotic factors (TGF-β, connective tissue growth factor) (Fig. 3*B*).

Erlotinib decreased urinary excretion of F2-isoprostane, a marker of oxidative stress (Fig. 4*A*). In addition, erlotinib decreased renal expression of CHOP, a marker of endoplasmic reticulum stress (Fig. 4*B*), and of 4-hydroxynonenal, another marker of oxidative stress (Fig. 4*C*).

Erlotinib treatment markedly decreased renal macrophage infiltration, as indicated by decreased F4/80 mRNA expression and decreased F4/80 staining (Fig. 4*D*). Erlotinib also decreased T-cell infiltration, as indicated by decreased CD3 mRNA and CD8α staining (Fig. 4*E*). Erlotinib treatment led to a significant decrease in mRNA for IRF5, a mediator of the proinflammatory M1 macrophage phenotype (20), and decreased mRNA for various proinflammatory cytokines (iNOS, TNF-α, INF-γ, IL-6) (Fig. 4*F*).

A striking finding in the erlotinib-treated mice was a relatively slow increase in body weight (body weight at 20 weeks 36.2 ± 1.5 g; 49.8 ± 1.4 g in mice receiving the vehicle; $P < 0.001$ [$n = 10$ mice in each group]) (Fig. 5*A*); this was due to smaller fat mass of erlotinib-treated mice (Supplementary Fig. 3). Erlotinib treatment also led to decreases in fasting blood glucose levels (blood glucose at 20 weeks: 124 ± 11; 568 ± 46 mg/dL in vehicle-treated mice; $P < 0.001$ [$n = 10$ mice in each group]) (Fig. 5*B*). The erlotinib-treated mice had improved glucose disposition and insulin sensitivity, as indicated by improvements in glucose tolerance test (Fig. 5*C*) and insulin tolerance test (Fig. 5*D*) results. In addition, the erlotinib-treated mice had preserved pancreatic islet insulin staining (Fig. 6*A*) and higher fasting blood insulin levels at 20 weeks (3.16 ± 0.31 vs. 1.88 ± 0.19 ng/mL in vehicle-treated mice; $P < 0.05$ [$n = 6$ mice in the 20-week groups]) (Fig. 6*B*). Erlotinib also decreased islet macrophage infiltration (Fig. 6*C*) and increased islet autophagy (Fig. 6*D*). Serum levels of adiponectin, an adipocyte-derived hormone that increases insulin sensitivity, decreased in vehicle-treated eNOS$^{-/-}$*db/db* mice at 20 weeks compared with values at 10 weeks, but erlotinib prevented this decrease (plasma adiponectin at 10 weeks: 21.44 ± 1.78 μg/mL [$n = 9$ mice]; at 20 weeks with vehicle treatment: 12.45 ± 1.02 μg/mL [$P < 0.001$ vs. the 10-week vehicle-treated group; $n = 12$ mice]; at 20 weeks with erlotinib: 20.57 ± 0.52 μg/mL [$P < 0.001$ vs. the 20-week vehicle-treated group; $n = 7$ mice]) (Fig. 6*E*). Erlotinib-mediated preservation of circulating adiponectin might protect against DN through activation of adiponectin receptors, although expression of these receptors was not increased in erlotinib-treated kidney (Supplementary Fig. 4).

As further confirmation of the role of EGFR activation in mediating diabetic kidney injury, we used *waved 2* mice, which have a point mutation in EGFR that reduces intrinsic tyrosine kinase activity by >90% (21). Compared to control (*wa2/+*;eNOS$^{-/-}$*db/db*) mice, homozygous *waved 2* mice crossed with eNOS$^{-/-}$*db/db* mice exhibited less body weight gain (Supplementary Fig. 5*A*), lower fasting blood glucose (Fig. 7*A*), less islet macrophage infiltration (Supplementary Fig. 6*A*), and less glomerulosclerosis (Fig. 7*E*) in association with preserved pancreatic insulin

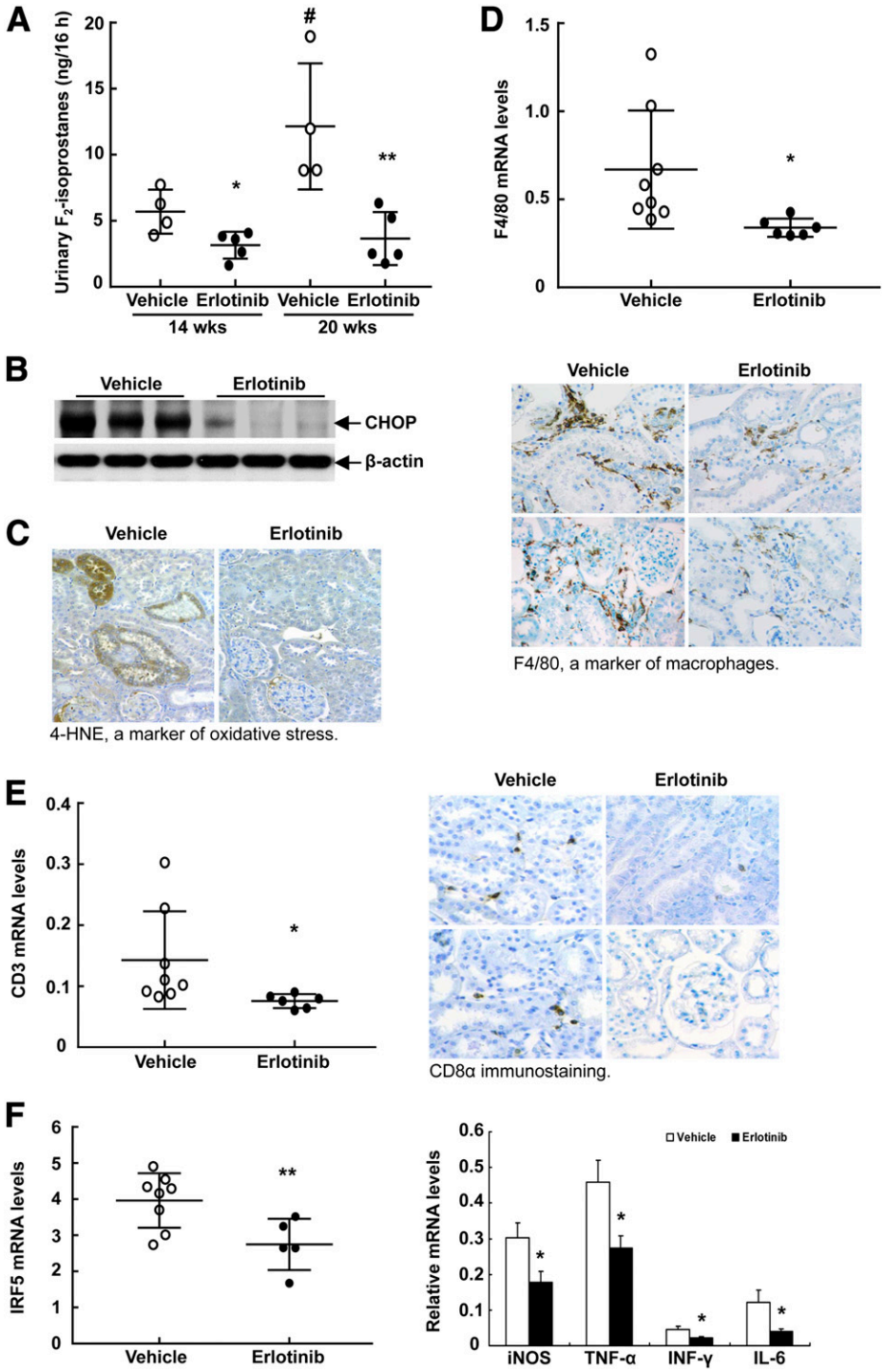

Figure 4— Erlotinib treatment decreased renal immune cell infiltration and oxidative stress. *A*: Urine was collected for 16 h and urinary excretion of F2-isoprostane, a biomarker of oxidative stress, was measured via gas chromatography–mass spectrometry. Urinary F2-isoprostane excretion markedly increased from 14 to 20 weeks; erlotinib administration caused excretion to decrease to low levels. $^{*}P < 0.05$, $^{**}P < 0.01$ vs. the corresponding vehicle-treated group; $^{\#}P < 0.05$ vs. the vehicle-treated group at 14 weeks ($n = 4$ mice in the vehicle-treated group and $n = 5$ mice in the erlotinib-treated group). *B*: Erlotinib decreased kidney endoplasmic reticulum, stress as indicated by CHOP immunoblotting. *C*: Erlotinib reduced renal oxidative stress, as indicated by decreases in 4-hydroxynonenal (4-HNE), a marker of oxidative stress. Original magnification ×300. *D*: Erlotinib treatment decreased renal macrophage infiltration, as indicated by decreased renal F4/80 mRNA levels (top) and immunostaining (bottom; original magnification ×300). $^{*}P < 0.05$ ($n = 8$ mice in the vehicle-treated group and $n = 6$ mice in the erlotinib-treated group). *E*: Erlotinib treatment decreased renal T-cell infiltration, as indicated by decreased renal CD3 mRNA levels (left) and CD8α immunostaining (right; original magnification ×300). $^{*}P < 0.05$ ($n = 8$ mice in the vehicle-treated group and $n = 6$ mice in the erlotinib-treated group). *F*: Erlotinib treatment decreased mRNA levels for the proinflammatory macrophage transcription factor IRF5 (left) and proinflammatory cytokines including iNOS, TNF-α, INF-γ, and IL-6 (right). $^{*}P < 0.05$, $^{**}P < 0.01$ ($n = 8$ mice in the vehicle-treated group and $n = 6$ mice in the erlotinib-treated group).

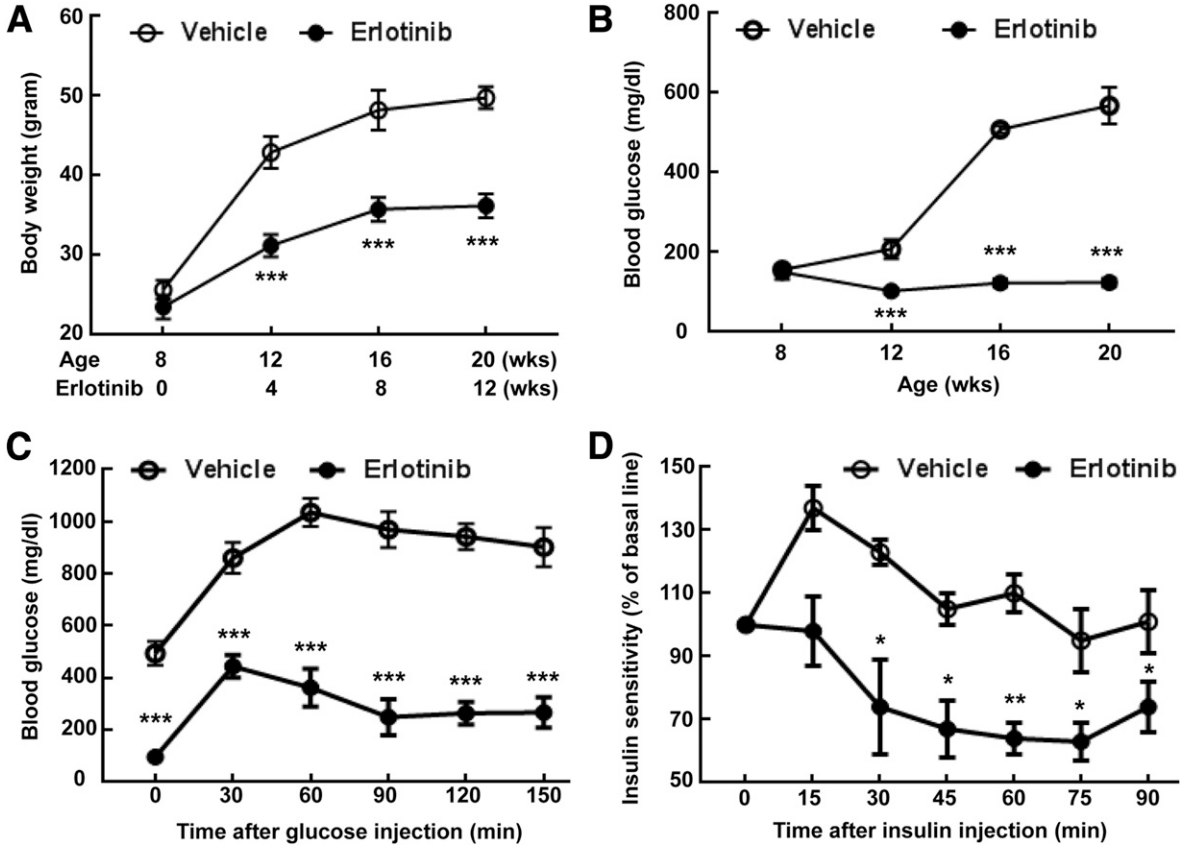

Figure 5—Erlotinib treatment decreased blood glucose and increased glucose tolerance and insulin sensitivity in eNOS$^{-/-}$*db/db* mice. *A*: Erlotinib treatment markedly attenuated body weight gain from 8 to 20 weeks in vehicle-treated eNOS$^{-/-}$*db/db* mice. ***$P < 0.001$ vs. the corresponding vehicle-treated group ($n = 10$ mice in each group). *B*: Erlotinib treatment prevented the progressive increases in blood glucose that occurred from 8 to 20 weeks in vehicle-treated eNOS$^{-/-}$*db/db* mice. ***$P < 0.001$ vs. the corresponding vehicle-treated group ($n = 10$ mice in each group). *C*: Erlotinib increased glucose tolerance by the end of treatment (from 8 to 20 weeks of age). ***$P < 0.001$ vs. the corresponding vehicle-treated group ($n = 6$ mice in the vehicle-treated group and $n = 5$ mice in the erlotinib-treated group). *D*: Erlotinib treatment increased insulin sensitivity. *$P < 0.05$, **$P < 0.01$ vs. the corresponding vehicle-treated group ($n = 4$ mice in the vehicle-treated group and $n = 5$ mice in the erlotinib-treated group).

production (Fig. 7*C*). Blood pressure was comparable between *waved 2* eNOS$^{-/-}$*db/db* mice and their controls (Supplementary Fig. 7). *Waved 1* mice have markedly decreased expression of TGF-α, an EGFR ligand (22). Similar to erlotinib-treated eNOS$^{-/-}$*db/db* and *waved 2* eNOS$^{-/-}$*db/db* mice, *waved 1* mice crossed with eNOS$^{-/-}$*db/db* mice also demonstrated marked decreases in body weight gain (Supplementary Fig. 5*B*), fasting blood glucose (Fig. 7*B*), islet macrophage infiltration (Supplementary Fig. 6*B*), and glomerulosclerosis (Fig. 7*F*), but had preserved pancreatic insulin levels (Fig. 7*D*).

Of note, eNOS$^{-/-}$*db/db* mice treated with erlotinib had markedly increased longevity compared with those mice that received the vehicle treatment (mean age at death 34.14 ± 1.18 vs. 22.08 ± 0.56 weeks; $P < 0.0001$ [$n = 8$ mice in each group]) (Fig. 8*A*).

DISCUSSION

Through the use of pharmacologic and genetic EGFR blockade, we investigated the potential role of EGFR activation in the development of DN in a model of accelerated type 2 diabetes, eNOS$^{-/-}$*db/db*. The major findings include the following: *1*) Inhibition of EGFR tyrosine kinase activity by erlotinib attenuated the progression of DN, as indicated by decreases in albuminuria, glomerulosclerosis, tubular injury, and fibrosis associated with decreased loss of podocytes. *2*) Erlotinib decreased renal macrophage and lymphocyte infiltration and oxidative stress. *3*) Erlotinib treatment led to decreases in body weight gain, fat tissue mass, and fasting blood glucose and increases in glucose tolerance, insulin sensitivity, and pancreatic insulin expression. *4*) Erlotinib increased circulating levels of adiponectin, an adipokine with insulin-sensitizing and kidney-protective effects. *5*) Erlotinib decreased systemic oxidative stress, as indicated by fewer F2-isoprostanes in the urine. *6*) Erlotinib treatment increased the longevity of eNOS$^{-/-}$*db/db* mice. *7*) The aforementioned effects of erlotinib were mimicked in mice with genetic EGFR inhibition with EGFR tyrosine kinase deficiency (*waved 2*) and in those lacking the EGFR ligand TGF-α (*waved 1*). The mechanisms underlying EGFR-mediated insulin resistance and DN are summarized in Fig. 8*B*.

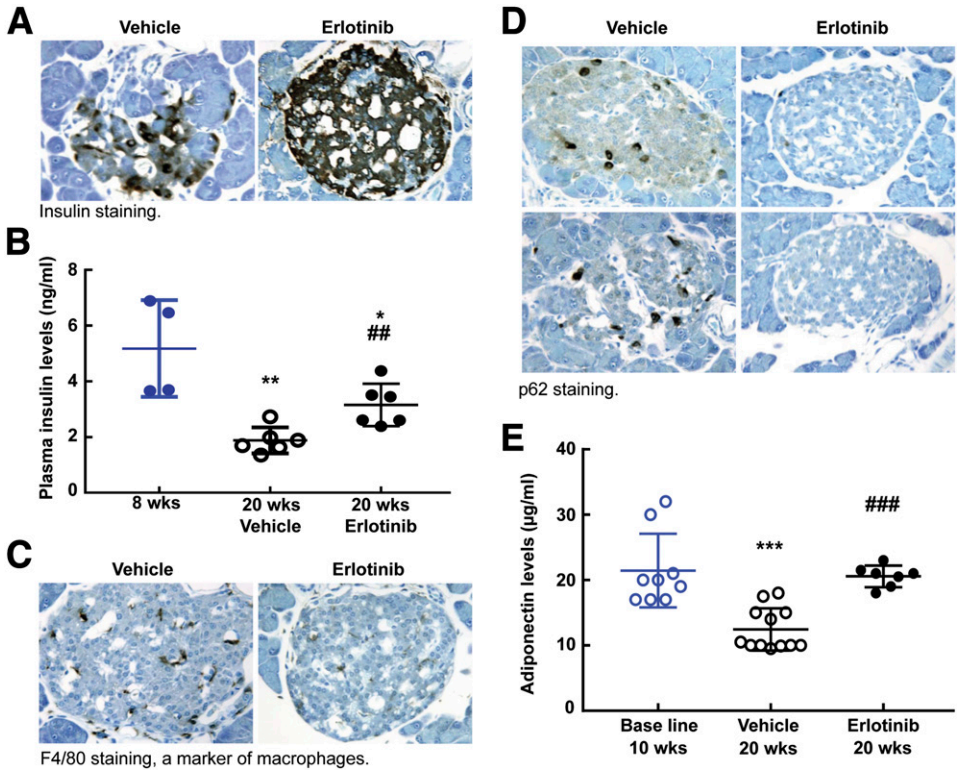

Figure 6—Erlotinib treatment protected insulin production and increased blood adiponectin levels. *A*: More intensive insulin staining was observed in islets from erlotinib-treated mice than in those from vehicle-treated mice (original magnification ×250). *B*: Erlotinib treatment attenuated marked decreases in fasting plasma insulin levels from 8 to 20 weeks in vehicle-treated eNOS$^{-/-}$*db/db*. *$P < 0.05$, **$P < 0.01$ vs. mice at 8 weeks, ##$P < 0.01$ vs. corresponding vehicle group ($n = 4$ in the 8-week group and $n = 6$ mice in both the vehicle- and the erlotinib-treated groups). *C* and *D*: Erlotinib treatment from 8 to 20 weeks in eNOS$^{-/-}$*db/db* mice decreased macrophage infiltration, as indicated by F4/80 immunostaining (*C*), and increased islet autophagy activity, as indicated by decreased expression of p62, a substrate of autophagy (*D*) (original magnification ×250). *E*: Erlotinib preserved circulating levels of the adipokine adiponectin. Adiponectin levels markedly decreased from 8 to 20 weeks in vehicle-treated eNOS$^{-/-}$*db/db* mice but were maintained at higher levels in erlotinib-treated mice. ***$P < 0.001$ vs. mice at 8 weeks, ###$P < 0.01$ vs. the corresponding vehicle-treated group ($n = 9$ mice in the 8-week group, $n = 12$ mice in the vehicle-treated group, and $n = 7$ mice in the erlotinib-treated group).

Studies from our laboratory and others support a role for EGFR activation as an important mediator of renal repair after acute injury (21,23,24). However, we and others have also ascribed to persistent EGFR activation a detrimental role in progressive renal fibrosis induced by subtotal nephrectomy (25), renovascular hypertension (26), angiotensin II (11,27), endothelin (28) or unilateral ureteral obstruction (29). Our recent study demonstrated that selective EGFR activation in the renal proximal tubule induces tubulointerstitial fibrosis, which can be attenuated with genetic or pharmacologic EGFR blockade (30). Our previous studies also indicated an important role for EGFR activation in mediating the development of DN in experimental type 1 diabetes (11–14). In preliminary studies with the use of gefitinib, a different EGFR inhibitor, we found protection against DN progression similar to that imparted by erlotinib. The current study indicates that EGFR blockade successfully inhibits the progression of DN, preserving glomerular structure and function and inhibiting tubulointerstitial fibrosis.

EGFR can be activated by a family of ligands, including epidermal growth factor, TGF-α, heparin-binding epidermal growth factor, betacellulin, amphiregulin, and epiregulin. Previous studies have suggested a potential role for TGF-α in mediating progressive renal injury. Laouari et al. (31) investigated the etiology of the documented susceptibility of FVB/N mice to chronic kidney injury and found evidence suggesting that increased TGF-α expression was a contributing factor. Heuer et al. (32) reported more recently that mAb41, a neutralizing monoclonal antibody with high affinity for TGF-α, slowed the progression of kidney injury in an accelerated model of DN. However, mAb41 also neutralizes epiregulin, another EGFR ligand, albeit at somewhat lower affinity (33). In the current study we used *waved 1* mice, which have markedly reduced TGF-α expression (22), and found significant protection against the development of DN in the eNOS$^{-/-}$*db/db* mice.

Although our previous studies clearly indicated that EGFR blockade directly inhibits the development of renal fibrotic injury in an insulinopenic model of accelerated type 1 diabetic nephropathy (12), we unexpectedly found that because of leptin receptor deficiency in this model of type 2 diabetes, erlotinib also preserved islet function, improved peripheral insulin sensitivity, and ameliorated

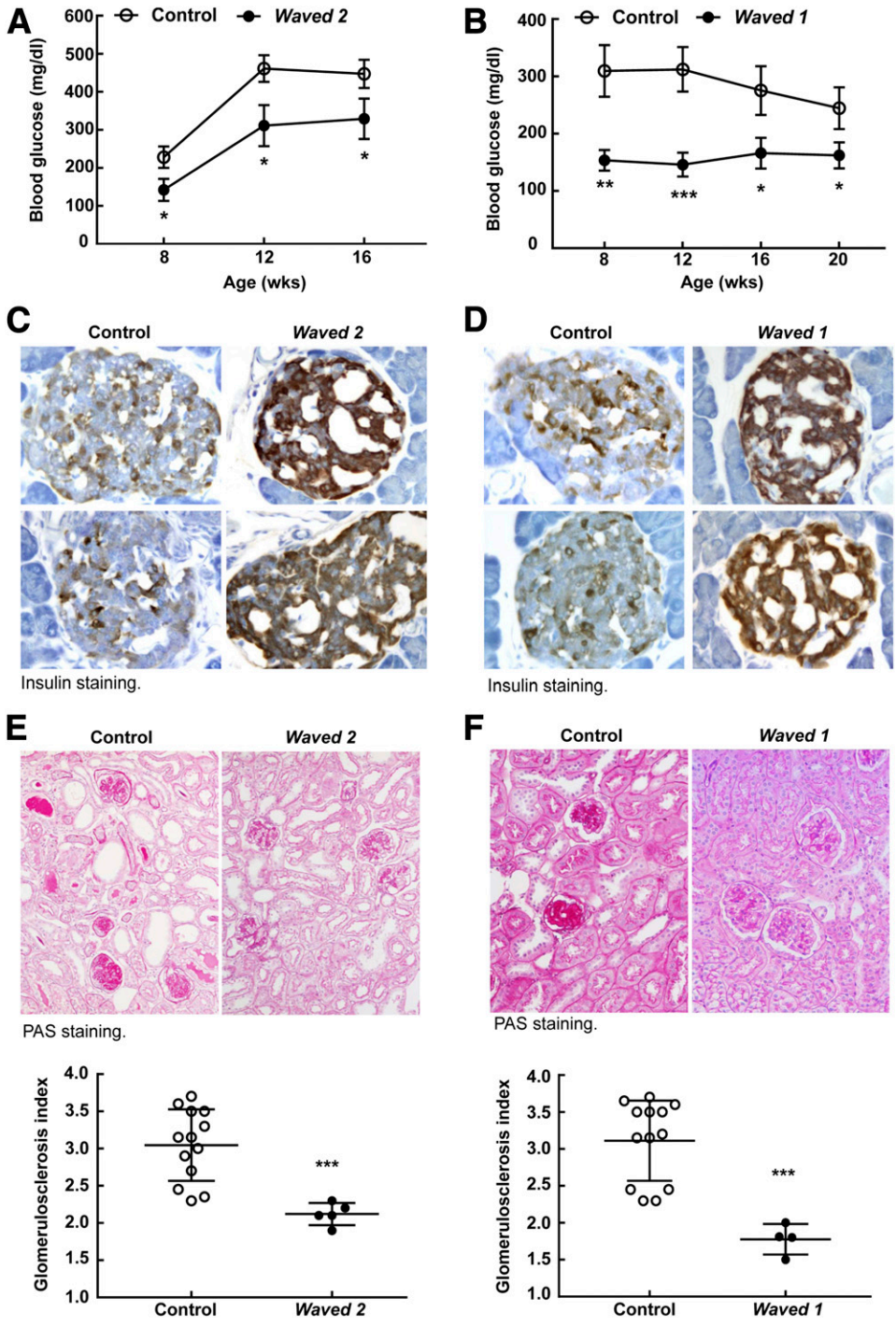

Figure 7—Genetic inhibition of the EGFR signaling pathway attenuated the development of DN in eNOS$^{-/-}$*db/db* mice. *A*: *Waved 2* eNOS$^{-/-}$*db/db* mice with EGFR tyrosine kinase deficiency had lower fasting blood glucose than control mice during development from 8 to 16 weeks of age. *$P < 0.05$ (n = 16 mice in each group). *B*: *Waved 1* eNOS$^{-/-}$*db/db* mice with null TGF-α showed lower fasting blood glucose than control mice during development from 8 to 20 weeks of age. *$P < 0.05$, **$P < 0.01$, ***$P < 0.001$ (n = 7 mice in the control group and n = 15 in the *waved 1* group). *C* and *D*: More intensive insulin staining was observed in islets from both *waved 2* eNOS$^{-/-}$*db/db* mice (*C*) and *waved 1* eNOS$^{-/-}$*db/db* mice (*D*) than in their corresponding controls (original magnification ×250). *E* and *F*: Both *waved 2* eNOS$^{-/-}$*db/db* mice (*E*) and *waved 1* eNOS$^{-/-}$ *db/db* mice (*F*) exhibited less glomerulosclerosis than did their corresponding controls, as indicated by periodic acid Schiff (PAS) staining (top; original magnification ×300) and glomerulosclerosis index (bottom). ***$P < 0.001$ (n = 5 mice in the *waved 2* group and n = 13 mice in its control group; n = 4 mice in the *waved 1* group and n = 13 mice in its control group).

weight gain. These findings are consistent with those from a report of relative improvement in glucose control in a patient with diabetes who was treated with erlotinib for lung cancer (34). EGFR blockade increases circulating insulin levels, and pancreatic insulin production may result from decreased islet macrophage infiltration and increased

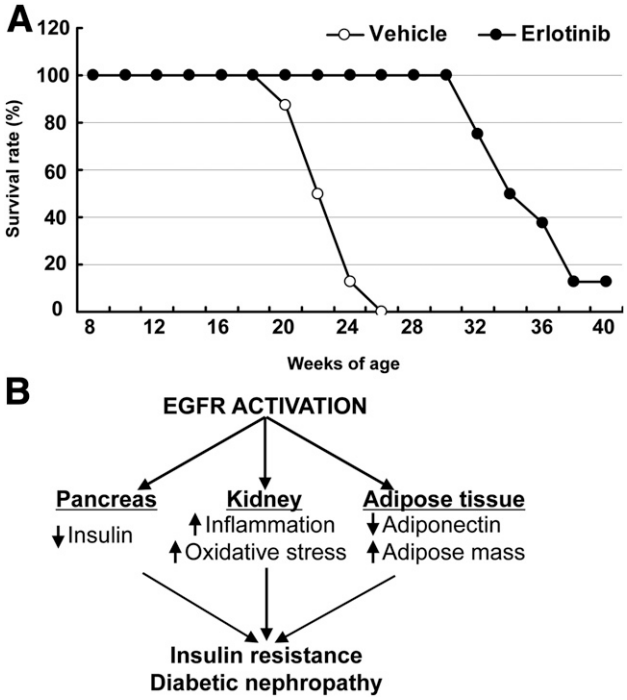

Figure 8— Erlotinib treatment increased the survival of eNOS$^{-/-}$*db/db* mice. *A*: Erlotinib treatment of eNOS$^{-/-}$*db/db* mice, initiated at the age of 8 weeks, markedly increased their longevity. *B*: EGFR activation increases immune cell infiltration and oxidative stress in the kidney and adipose mass, but decreases pancreatic insulin production and adipocyte adiponectin production, leading to insulin resistance and DN in type 2 diabetes.

islet autophagy, leading to preserved islet structure and function. Autophagy is a major regulator of β-cell insulin homeostasis (35). Using mice with autophagy deficiency in β-cells (Atg7, deletion of autophagy-related 7), Jung et al. (36) determined that autophagy plays a key role in maintaining pancreatic β-cell structure, mass, and function. Autophagy deficiency in pancreatic β-cells may contribute to the progression from obesity to diabetes (37). Erlotinib treatment may also increase insulin sensitivity by preserving circulating levels of adiponectin, an insulin-sensitizing and anti-inflammatory adipokine produced by adipocytes.

Preservation of circulating adiponectin levels should be considered among the mechanism(s) contributing to the kidney-protective effect seen with EGFR inhibition. Adiponectin has been shown to be renoprotective in different kidney injury models and after podocyte injury (38,39). It protects against hypoxia-induced kidney injury by inhibiting endoplasmic reticulum stress (40). It also inhibits the TGF-β signaling pathway, and its deletion leads to increases in renal fibrosis and inflammation in diabetic mice (41). In addition, adiponectin protect against islet ischemic injury (42). Circulating adiponectin concentrations are reduced in obesity. In this regard, circulating adiponectin levels markedly decreased in eNOS$^{-/-}$*db/db* mice from 8 to 20 weeks of age, and this decrease was prevented with erlotinib treatment.

In summary, the mechanisms mediating the beneficial effects of EGFR blockade on DN are multifactorial. *1*) EGFR blockade may directly protect against DN by inhibiting renal immune cell infiltration and oxidative stress, thereby decreasing the expression of profibrotic and fibrotic components. *2*) EGFR blockade may also indirectly protect against DN by increasing islet autophagy activity, leading to preservation of pancreatic β-cell function and subsequent improvement of metabolic status. *3*) EGFR blockade increases circulating levels of the adipokine adiponectin, which has insulin-sensitizing, anti-inflammatory, and kidney-protective effects. *4*) EGFR blockade decreases systemic oxidative stress, as indicated by decreased urinary F2-isoprostanes, which are a well-accepted marker of systemic oxidative stress. Further study is required to determine all of the mechanisms underlying the amelioration of diabetes through EGFR inhibition. Although EGFR inhibitors have known side effects—notably skin rash—that might limit their long-term use in humans with diabetic kidney disease, downstream signaling pathways activated by EGFR may be attractive targets for future therapeutic interventions.

Funding. This work was supported by the National Institutes of Health National Institute of Diabetes and Digestive and Kidney Diseases (grant nos. DK051265 to M.-Z.Z. and R.C.H., DK062794 to R.C.H., DK095785 to M.-Z.Z. and R.C.H.), by the Vanderbilt O'Brien Kidney Center (grant no. DK114809 to M.-Z.Z. and R.C.H.), and by funds from the U.S. Department of Veterans Affairs (to R.C.H.).

Duality of Interest. No potential conflicts of interest relevant to this article were reported.

Author Contributions. Z.L., Y.L., J.M.O., S.C., A.N., X.F., S.W., and Y.W. performed the experiments. M.-Z.Z. and R.C.H. designed the study, performed the experiments, and wrote the manuscript. R.C.H. is the guarantor of this work and, as such, had full access to all the data in the study and takes responsibility for the integrity of the data and the accuracy of the data analysis.

References

1. Donate-Correa J, Martin-Nuñez E, Muros-de-Fuentes M, Mora-Fernández C, Navarro-González JF. Inflammatory cytokines in diabetic nephropathy. J Diabetes Res 2015;2015:948417
2. Zha D, Wu X, Gao P. Adiponectin and its receptors in diabetic kidney disease: molecular mechanisms and clinical potential. Endocrinology 2017;158:2022–2034
3. Chang AS, Hathaway CK, Smithies O, Kakoki M. Transforming growth factor-β1 and diabetic nephropathy. Am J Physiol Renal Physiol 2016;310:F689–F696
4. Yamout H, Lazich I, Bakris GL. Blood pressure, hypertension, RAAS blockade, and drug therapy in diabetic kidney disease. Adv Chronic Kidney Dis 2014;21:281–286
5. Schlessinger J. Ligand-induced, receptor-mediated dimerization and activation of EGF receptor. Cell 2002;110:669–672
6. Hynes NE, Lane HA. ERBB receptors and cancer: the complexity of targeted inhibitors. Nat Rev Cancer 2005;5:341–354
7. Yarden Y, Sliwkowski MX. Untangling the ErbB signalling network. Nat Rev Mol Cell Biol 2001;2:127–137
8. Harris RC. Response of rat inner medullary collecting duct to epidermal growth factor. Am J Physiol 1989;256(6 Pt 2):F1117–F1124
9. Harris RC, Hoover RL, Jacobson HR, Badr KF. Evidence for glomerular actions of epidermal growth factor in the rat. J Clin Invest 1988;82:1028–1039
10. Breyer MD, Redha R, Breyer JA. Segmental distribution of epidermal growth factor binding sites in rabbit nephron. Am J Physiol 1990;259:F553–F558

11. Chen J, Chen JK, Nagai K, et al. EGFR signaling promotes TGFβ-dependent renal fibrosis. J Am Soc Nephrol 2012;23:215–224
12. Zhang MZ, Wang Y, Paueksakon P, Harris RC. Epidermal growth factor receptor inhibition slows progression of diabetic nephropathy in association with a decrease in endoplasmic reticulum stress and an increase in autophagy. Diabetes 2014;63:2063–2072
13. Chen J, Chen JK, Harris RC. EGF receptor deletion in podocytes attenuates diabetic nephropathy. J Am Soc Nephrol 2015;26:1115–1125
14. Chen J, Harris RC. Interaction of the EGF receptor and the hippo pathway in the diabetic kidney. J Am Soc Nephrol 2016;27:1689–1700
15. Zhao HJ, Wang S, Cheng H, et al. Endothelial nitric oxide synthase deficiency produces accelerated nephropathy in diabetic mice. J Am Soc Nephrol 2006;17:2664–2669
16. Yao B, Harris RC, Zhang MZ. Intrarenal dopamine attenuates deoxycorticosterone acetate/high salt-induced blood pressure elevation in part through activation of a medullary cyclooxygenase 2 pathway. Hypertension 2009;54:1077–1083
17. Morrow JD, Roberts LJ. The isoprostanes: unique bioactive products of lipid peroxidation. Prog Lipid Res 1997;36:1–21
18. Zhang MZ, Wang JL, Cheng HF, Harris RC, McKanna JA. Cyclooxygenase-2 in rat nephron development. Am J Physiol 1997;273:F994–F1002
19. Zhang MZ, Wang S, Yang S, et al. Role of blood pressure and the renin-angiotensin system in development of diabetic nephropathy (DN) in eNOS-/-db/db mice. Am J Physiol Renal Physiol 2012;302:F433–F438
20. Weiss M, Byrne AJ, Blazek K, et al. IRF5 controls both acute and chronic inflammation. Proc Natl Acad Sci U S A 2015;112:11001–11006
21. Wang Z, Chen JK, Wang SW, Moeckel G, Harris RC. Importance of functional EGF receptors in recovery from acute nephrotoxic injury. J Am Soc Nephrol 2003;14:3147–3154
22. Berkowitz EA, Seroogy KB, Schroeder JA, et al. Characterization of the mouse transforming growth factor alpha gene: its expression during eyelid development and in waved 1 tissues. Cell Growth Differ 1996;7:1271–1282
23. Hirschberg R, Ding H. Growth factors and acute renal failure. Semin Nephrol 1998;18:191–207
24. Chen J, Chen JK, Harris RC. Deletion of the epidermal growth factor receptor in renal proximal tubule epithelial cells delays recovery from acute kidney injury. Kidney Int 2012;82:45–52
25. Terzi F, Burtin M, Hekmati M, et al. Targeted expression of a dominant-negative EGF-R in the kidney reduces tubulo-interstitial lesions after renal injury. J Clin Invest 2000;106:225–234
26. François H, Placier S, Flamant M, et al. Prevention of renal vascular and glomerular fibrosis by epidermal growth factor receptor inhibition. FASEB J 2004;18:926–928
27. Lautrette A, Li S, Alili R, et al. Angiotensin II and EGF receptor cross-talk in chronic kidney diseases: a new therapeutic approach. Nat Med 2005;11:867–874
28. Chansel D, Ciroldi M, Vandermeersch S, et al. Heparin binding EGF is necessary for vasospastic response to endothelin. FASEB J 2006;20:1936–1938
29. Liu N, Guo JK, Pang M, et al. Genetic or pharmacologic blockade of EGFR inhibits renal fibrosis. J Am Soc Nephrol 2012;23:854–867
30. Overstreet JM, Wang Y, Wang X, et al. Selective activation of epidermal growth factor receptor in renal proximal tubule induces tubulointerstitial fibrosis. FASEB J 2017;31:4407–4421
31. Laouari D, Burtin M, Phelep A, et al. TGF-alpha mediates genetic susceptibility to chronic kidney disease. J Am Soc Nephrol 2011;22:327–335
32. Heuer JG, Harlan SM, Yang DD, et al. Role of TGF-alpha in the progression of diabetic kidney disease. Am J Physiol Renal Physiol 2017;312:F951–F962
33. Beidler CB, Petrovan RJ, Conner EM, et al. Generation and activity of a humanized monoclonal antibody that selectively neutralizes the epidermal growth factor receptor ligands transforming growth factor-α and epiregulin. J Pharmacol Exp Ther 2014;349:330–343
34. Costa DB, Huberman MS. Improvement of type 2 diabetes in a lung cancer patient treated with erlotinib. Diabetes Care 2006;29:1711
35. Riahi Y, Wikstrom JD, Bachar-Wikstrom E, et al. Autophagy is a major regulator of beta cell insulin homeostasis. Diabetologia 2016;59:1480–1491
36. Jung HS, Chung KW, Won Kim J, et al. Loss of autophagy diminishes pancreatic beta cell mass and function with resultant hyperglycemia. Cell Metab 2008;8:318–324
37. Quan W, Hur KY, Lim Y, et al. Autophagy deficiency in beta cells leads to compromised unfolded protein response and progression from obesity to diabetes in mice. Diabetologia 2012;55:392–403
38. Ding W, Cai Y, Wang W, et al. Adiponectin protects the kidney against chronic intermittent hypoxia-induced injury through inhibiting endoplasmic reticulum stress. Sleep Breath 2016;20:1069–1074
39. Fang F, Bae EH, Hu A, et al. Deletion of the gene for adiponectin accelerates diabetic nephropathy in the Ins2 (+/C96Y) mouse. Diabetologia 2015;58:1668–1678
40. Rutkowski JM, Wang ZV, Park AS, et al. Adiponectin promotes functional recovery after podocyte ablation. J Am Soc Nephrol 2013;24:268–282
41. Sharma K, Ramachandrarao S, Qiu G, et al. Adiponectin regulates albuminuria and podocyte function in mice. J Clin Invest 2008;118:1645–1656
42. Du X, He S, Jiang Y, Wei L, Hu W. Adiponectin prevents islet ischemia-reperfusion injury through the COX2-TNFα-NF-κB-dependent signal transduction pathway in mice. J Endocrinol 2013;218:75–84